

Film structure and enhanced superconductivity in evaporated aluminum films*

Richard B. Pettit

Sandia Laboratories, Albuquerque, New Mexico 87115

J. Silcox

School of Applied and Engineering Physics, Cornell University, Ithaca, New York 14850

(Received 31 October 1974; revised manuscript received 8 December 1975)

The increase in the superconducting transition temperature of evaporated aluminum films is correlated with the following structural properties of the films: the average grain size, the average lattice constant, the film thickness, and the presence or absence of a thin oxide layer surrounding each grain in the film. It is found that for all the films studied, the transition temperature T_c is a function only of the average grain size a with $\ln(T_c) \propto a^{-0.82}$. This approximate $1/a$ dependence is in agreement with several theories which indicate that the increased transition temperatures result from changes in the phonon spectrum at the surface of small grains. Even though we have determined that there is a thin oxide layer surrounding each grain in several films, an electron-exciton-electron enhancement mechanism that has been proposed is not observed. However, the presence of the oxide may influence the magnitude of the enhancement.

I. INTRODUCTION

Many materials, including Al, Ga, In, Mo, Re, Sr, Tl, W, and Zr, show enhanced critical temperatures under a variety of conditions,¹⁻³ for example, as thin films. The present study concentrates on this enhancement in evaporated aluminum films. Previous experimental investigations have demonstrated a variety of procedures which produce aluminum films with enhanced critical temperatures. This includes the evaporation of aluminum onto helium-cooled substrates,^{1,4,5} in the presence of a background partial pressure of oxygen,^{2,6} or together with a dielectric,⁷⁻¹⁰ or with another metal.¹¹ Experimentally, the enhancement has been related to the average grain size,^{2,4-6} the film thickness,¹² dielectric barriers or coatings,^{2,8,13,14} and changes in the crystal lattice constant.¹⁵ Theoretically, the enhancement has been attributed to the quantization of electron levels in small grains,¹⁶ dielectric coatings or barriers,¹⁷⁻¹⁹ and changes in the phonon spectrum at the surface of small crystallites.^{17,20,21}

Disorder in these films has been identified²² as the most likely origin of the observed increases in T_c , but effective characterization of disorder is not always easy to accomplish. Recently, we reported²³ an extensive study of the structural characteristics of a range of aluminum films in which particular attention was paid to the presence or absence of an oxide structure at the grain boundaries in the films. Other important structural properties determined included the average grain size, the average lattice constant, and the film thickness. Our results indicate that the increase in the transition temperature is inversely proportional to the average grain size a over the

range $160 \geq a \geq 50$ Å. This grain size dependence is in agreement with several theories which indicate that the increase in the transition temperature is a result of changes in the phonon spectrum at the surface of small grains. Numerical values for the parameters involved in the theory are obtained.

II. EXPERIMENTAL AND THEORETICAL BACKGROUND

Although the first observation of an increase in the transition temperature T_c in aluminum and other materials was for films deposited on liquid-helium-cooled substrates,¹ a rise in T_c has been found for aluminum using a variety of experimental techniques.¹⁻¹² Most recent experimental evidence indicates that the T_c increases results from changes in the electron-phonon (el-ph) coupling at the surface of thin films or small grains.^{5,6,11,13,22} In particular, the increase in T_c for layered metallic films¹¹ agrees with predictions based on a shift in the el-ph coupling at the metal interface. In addition, both Deutscher *et al.*⁶ and Watton⁵ demonstrated, for aluminum, that T_c increased as the grain size decreased in agreement with the same el-ph enhancement mechanism. Finally, Naugle *et al.*¹³ measured a decrease in T_c for aluminum films coated with an overlayer of Ne or Ar. The results were again consistent with a modified phonon spectrum at the aluminum film surface, caused by the noble gas. This el-ph enhancement mechanism can also be used to explain the enhancement observed in all other experimental results, except possibly the work of Hauser,¹⁵ where the observed enhancement was accounted for by a corresponding increase in the average lattice constant of each film. One other inves-

tigation⁶ measured the lattice parameter of each film but found no increase over that of bulk aluminum.

Theoretically, the increase in the transition temperature has been related to disorder in prepared samples, or to an enhancement in a very thin layer near the surface of a film or a grain. Parmenter¹⁶ considered the quantization of electron levels in small grains to predict that

$$\alpha \ln \alpha = 1.385 (L/a)^3, \quad (1)$$

where α is the ratio of the enhanced transition temperature to the bulk transition temperature ($\alpha = T_c/T_{c0}$) and $L = 62 \text{ \AA}$ for aluminum. Subsequently, Strongin, Thompson, Kammerer, and Crow²⁴ have shown that the critical temperature should decrease as a result of quantization.

Hurault¹⁷ studied the superconducting properties of small metallic crystallites surrounded by a polarizable material. In the vicinity of the crystallite surface, the phonon spectrum is modified, which leads to an enhancement such that $\ln \alpha$ is inversely proportional to the particle size, i. e., $\ln \alpha \propto 1/a$. The polarizable material, if it is present, may contribute an extra electron-electron attractive interaction via a polarization wave, which leads to an enhancement such that $\ln \alpha$ is inversely proportional to the grain size squared, i. e., $\ln \alpha \propto 1/a^2$. Because of the different grain size dependences, it becomes possible to distinguish between the two proposed enhancement mechanisms. If both mechanisms are important, then $\ln \alpha$ should vary as $1/a$ for large values of a , and as $1/a^2$ for small values of a , i. e., $a \leq 50 \text{ \AA}$. However, the polarization mechanism seems unlikely, according to the analysis of Allender, Bray, and Bardeen²⁵ since aluminum oxide has a relatively large band gap ($\sim 7 \text{ eV}$).²⁶

Garland *et al.*²⁰ considered the effect of disorder on the superconducting transition temperature. For films composed of small crystalline grains, the average amplitude of ionic vibrations increases while the frequency of the vibrations is lowered. This leads to a decrease in the average phonon frequency, $\langle \omega_{\text{ph}} \rangle$, which increases T_c , and to a broadening of the peak in the phonon density of states $D(\omega)$, which decreases T_c . The complete theory, together with a modification by Watton,⁵ leads to an initial dependence of $\ln \alpha$, which is proportional to $1/a$. However, as the grain size continues to decrease, $\ln \alpha$ reaches a maximum and then falls sharply, indicating a decrease in the transition temperature. This theory will be discussed further in a later section. However, it should be mentioned that a functional relationship between $\ln \alpha$ and the grain size is predicted with only one adjustable parameter.

In general, then, one expects the transition temperature to be enhanced in thin films or in superconductors composed of small grains. Experimentally, the enhancement appears to be a result of changes in the el-ph coupling at the surface of thin films or small grains. However, the role of any dielectric or oxide barriers in the films, if they are present, is still unclear.^{6,13}

III. EXPERIMENTAL PROCEDURE

Aluminum films were deposited in an evaporation chamber that was designed to allow several evaporation conditions: (i) Evaporation onto a room-temperature substrate with a variable background pressure of air; (ii) evaporation onto a room-temperature substrate with a variable background pressure of oxygen; and (iii) evaporation onto a liquid-nitrogen-cooled substrate with a background pressure of air. The evaporation system has been previously described.²³

A mechanical shutter between the substrate and the evaporator allowed a constant evaporation rate to be established before the substrate was exposed to the vapor beam. By shielding one-half of the substrate with the shutter, approximately half-way through an evaporation, two specimens identical except in thickness were obtained. The thinner specimen, usually about 350 \AA thick, was stripped and mounted for examination in an electron microscope.

The substrate was a glass microscope slide fitted with indium contact points for holding electrical wires, and ultrasonically cleaned before being mounted in the evaporator. All films were scratched with a sharp needle for four-terminal resistance measurements, with the usual width to length ratio being 1:6. It was hoped that the trimming procedure would eliminate any effects due to tapered edges.

The superconductivity measurements were performed in an Andonian stainless-steel Dewar with a narrow 1-in.-i.d. tail section. The temperature was varied by pumping on the ⁴He bath with two large mechanical pumps; the lowest obtainable temperature was 1.17 K. A germanium resistance thermometer was calibrated against the vapor pressure of ⁴He, using the 1958 ⁴He temperature scale.²⁷ The resulting resistance calibration curve was a least-mean-squares curve fit to the formula $R_0 e^{5/T} + R_1$, with an accuracy of $\pm 5 \text{ mK}$, which is the reproducibility of the thermometer with thermal cycling.

The transition temperature of each film was determined with a constant current flowing through the film (usual current densities were less than 1 A/cm^2). No voltage drop along the specimen could be measured far below the transition temperature. As the temperature was increased, a

voltage gradually appeared along the specimen. The transition temperature was then determined by fitting approximately the upper 5% of this transition to the theory of Aslamazov and Larkin.^{28,29} This theory predicts for a film of thickness d with $T > T_c$ that

$$G(T) \left(\frac{R(T)}{R_N - R(T)} \right) = \frac{1}{\tau_0} \left(\frac{T - T_c}{T_c} \right), \quad (2)$$

with

$$G(T) = \frac{1}{2} \left(1 + \frac{d}{\xi(T)} \coth \frac{d}{\xi(T)} \right),$$

where $\xi(T)$ is the coherence length, $R(T)$ is the measured film resistance at a temperature T , and R_N is the normal resistance of the film. Extrapolation of the resulting straight line to the point where $R(T) = 0$ determines the critical temperature T_c . Previous experimental studies had indicated that the normal resistance R_N in some cases may also be temperature dependent for tem-

peratures near T_c .²⁹ Therefore, $R_N(T)$ was measured at temperatures above the transition temperature by applying a large perpendicular magnetic field which suppressed all superconductivity in the film. This field was produced by a Magnion magnet positioned around the tail section of the Dewar. The applied field was known to $\pm \frac{1}{4}$ Oe at $H=0$ and to 0.1% or 1.0 Oe at high fields. The magnet was also used to study the perpendicular upper critical field as a function of temperature for several films.

Transmission electron microscopy and lattice diffraction studies were carried out on a Siemens Elmiskop 1A electron microscope. Examples taken from these studies on the identical films considered here are available elsewhere.²³ For ease of measurement, the lattice parameter for each film was determined relative to a very clean aluminum film (film Al 146) which had a transition temperature only 0.04 K above the bulk value of 1.19 K. It was therefore assumed that the lattice

TABLE I. Properties of evaporated aluminum films.

Film	Thickness (Å)	Condensation rate (Å/sec)	Temperature of substrate ^b	Condensation pressure (Torr)	Lattice constant (Å)	Grain size (Å)	R_N^a, Ω^b	$10^5 \tau_0$	t	T_c (K)
Al 61	500	0.54	R. T.	1.3×10^{-6} air	4.061	160	1.3	34.	0.28	1.47
Al 135	750 380	10.0	R. T.	5×10^{-4} air	4.055	167	*** 0.63	*** 7.7	0.51	1.42 1.44
Al 133 ^a	770 380	7.0	R. T.	5×10^{-4} air	4.061	126	0.5 1.0	5.8 5.7	0.47	1.55 1.57
Al 132	745 380	5.1	R. T.	5.4×10^{-4} air	4.062	90	0.55 1.4	11. 20.	0.50	1.63 1.62
Al 131 ^a	755 380	3.9	R. T.	5.5×10^{-4} air	4.058	81	0.92 1.80	16. 18.	0.43	1.67 1.72
Al 130	720 390	2.4	R. T.	5.8×10^{-4} air	4.060	40	5.9 15.	*** 120.	0.17	1.98 2.02
Al 141	890 460	12.0	R. T.	5×10^{-5} O ₂	4.051	77	1.4 2.8	*** 28.	0.30	*** 1.83
Al 137 ^a	1400 700	13.0	R. T.	1.4×10^{-5} O ₂	4.064	64	0.79 1.9	*** 5.6	0.35	*** 1.88
Al 143	605 295	6.5	R. T.	6.2×10^{-5} O ₂	4.067	40	5.8 12.	93. ***	0.23	2.09 ***
Al 120 ^a	720 355	2.0	105 K	1.2×10^{-6} air	4.049	66	3.8 11.	*** 120.	0.16	*** 2.11
Al 125 ^a	730 375	3.4	95 K	2×10^{-6} air	4.069	59	3.3 6.4	26. 53.	0.23	2.00 2.00
Al 117 ^a	675 360	1.9	110 K	1.2×10^{-6} air	4.064	50	6.2 18.	34. 160.	0.13	2.22 2.37
Al 146	980	***	R. T.	2×10^{-6} air	4.050 (assumed)	***	0.079	2.5	***	1.23

^aIndicates that the oxide structure was definitely present in these films.

^bR. T. means room temperature; $R_N^a = \rho_N / a$.

constant of this film equaled the bulk value of 4.050 Å. The measurement accuracy of this technique was $\pm 0.5\%$.

The average grain size of each film was determined from the full width at half-height of the (111) diffraction ring as previously described.²³ The effect of strains in broadening the diffraction peaks was minimal and has been neglected. Values of the lattice parameter and grain size are given in Table I.

IV. RESULTS AND DISCUSSION

A. Superconducting properties

As previously discussed, the transition temperature of each film was determined by fitting the resistive transition for temperatures above T_c to Eq. (2). For all the films reported in this paper, the normal resistance R_N was constant to within one part in 10^4 for temperatures near T_c . The linear temperature dependence of Eq. (2) was found to hold only for approximately the upper 3% of the resistive transition for each film,

in agreement with previous results.²⁹ The critical temperatures determined in this way for each film are listed in Table I together with the structural parameters and the values of R_N and τ_0 for each film.

The difference between the critical temperature of the thick and thin films was usually less than 40 mK, with the notable exceptions being Al 120, (130 mK difference) and Al 117 (150 mK difference). However, in all cases, T_c for the thin film was higher than T_c for the thick film, indicating a slight film thickness dependence. The transition temperatures determined in this way differed by only ± 10 mK from the transition temperatures defined by the condition $R/R_N = \frac{1}{2}$.

Our experimental values of τ_0 [see Eq. (2)] are in agreement with the previous work of Masker and Parks²⁹ and Bhatnager *et al.*³⁰ The films of Masker and Parks²⁹ were evaporated in the presence of oxygen onto room-temperature glass substrates, while Bhatnager *et al.*³⁰ prepared their films by the evaporation of aluminum onto liquid-nitrogen-cooled glass substrates.

It has been shown³¹ that electrical transport in a system of metallic grains separated by δ -function tunneling barriers of transmission coefficient t is characterized by an effective mean free path l_{eff} ,

$$l_{\text{eff}} = at/(1-t) \quad (3)$$

This model has been applied to granular aluminum films in order to determine a value for the tunneling coefficient t . The effective mean free path is easily determined from the temperature dependence of the perpendicular critical magnetic field, which for aluminum,

$$H_L = 2.3 \times 10^{-4} \left(\frac{T_c - T}{l_{\text{eff}}} \right) \text{ G cm/K} \quad (4)$$

The perpendicular critical magnetic field was determined from the resistive transition at constant temperature as a function of the applied field. A typical transition is shown in Fig. 1(a). In agreement with Abeles *et al.*³¹ we have chosen the point where $R/R_N = 0.5$ as determining the critical field. However, it should be noted that the width of the transition is approximately 20% of the critical field. As shown in Fig. 1(b), the critical field determined in this way is a linear function of the temperature, in agreement with Eq. (4). Listed in Table II are the values of l_{eff} , determined for several films. From our data, which are limited to films with a mean free path in the range 7–12 Å, we find

$$\rho_N l_{\text{eff}} \cong 3.5 \times 10^{-12} \text{ } \Omega \text{ cm}^2 \quad (5)$$

where ρ_N is the resistivity in the normal state. This is compared to a value $\sim 7 \times 10^{-12} \text{ } \Omega \text{ cm}^2$ found

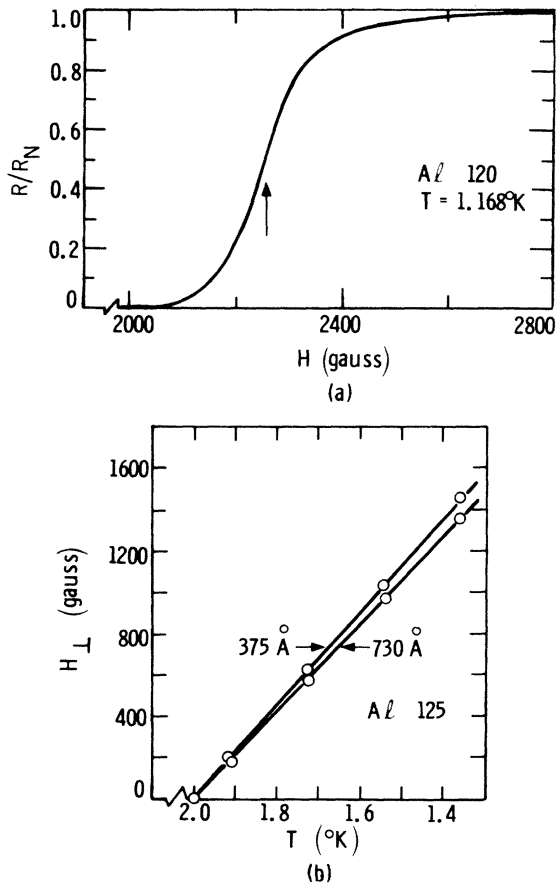


FIG. 1. Typical magnetic field transition at constant temperature and the perpendicular critical field as a function of temperature.

TABLE II. Quantity ρl for several evaporated aluminum films.

Film	Thickness (\AA)	$\rho l (\Omega \text{ cm}^2)$	$l (\text{\AA})$
Al 120	720	3.3×10^{-12}	12.0
	355	3.7×10^{-12}	9.3
Al 125	730	2.7×10^{-12}	11.0
	375	2.4×10^{-12}	9.7
Al 117	675	4.1×10^{-12}	9.6
	360	4.7×10^{-12}	7.3

by Abeles *et al.*,³¹ while Hauser³² obtained a value $\cong 5 \times 10^{-12} \Omega \text{ cm}^2$ for the same range of l_{eff} . Previous measurements of ρl for bulk aluminum range from 16×10^{-12} to $4.2 \times 10^{-12} \Omega \text{ cm}^2$. Our result agrees approximately with the lower value of $4.2 \times 10^{-12} \Omega \text{ cm}^2$.

The barrier transmission coefficients t , calculated from Eq. (3), are listed in Table I. We have used the value $\rho l = 4.2 \times 10^{-12} \Omega \text{ cm}^2$ to calculate the mean free path for each film. The values for t are very large, indicating that the grains are strongly coupled to each other, which is in agreement with previous results.³¹ However, from Table I, one can see that generally, as the transmission coefficient decreases, the critical temperature increases.

B. Film structure

We have previously shown that under all the evaporation conditions described above, aluminum films can be deposited that have a thin oxide layer surrounding each grain.²³ Very little indication of this unusual microstructure is observed from focused transmission micrographs, probably because the oxide thickness is less than $\approx 20 \text{\AA}$. However, the presence of the foreign material in the film is easily determined from the appearance of a regular Fresnel fringe pattern in slightly out-of-focus transmission micrographs, and the presence of a diffraction ring in the small-angle diffraction pattern.

The presence of this structure appears to be sensitive to the evaporation rate, the background pressure of air or oxygen, and the substrate temperature, although we have only determined general trends for these parameters.²³ The films in which an oxide structure has definitely been found are indicated in Table I. This includes six out of the ten films with a transition temperature equal to 1.55 K or greater. Because of the agreement between our values of τ_0 and the data of both Masker and Parks²⁹ and Bhatnager *et al.*,³⁰ we feel that their films should also have similar structural properties. This should also include all films grown under similar evaporation con-

ditions. The role of the oxide in determining the superconducting properties will be discussed later.

The measured lattice constant of each film agrees with the lattice constant of the reference film Al 146 to within experimental errors (see Table I). For aluminum, the measured value for the change in T_c per unit strain is -66 K .³³ Thus, aluminum under compression has a lower T_c , while aluminum under tension has a higher T_c . Our measurement accuracy of the lattice constant of $\pm 0.5\%$ corresponds to a T_c uncertainty of $\pm 0.33 \text{ K}$. Therefore, in films with a transition temperature above 1.52 K, a change in the lattice constant would become measurable, assuming that all of the increase is due to changes in the lattice constant. Accordingly, the measured increase in T_c for ten of the twelve films listed in Table I cannot be accounted for by strains in the lattice. Thus, it appears that any oxygen trapped in the films does not appreciably change the lattice constant. This is in contrast with the results of Hauser¹⁵ where a maximum of 3.5% increase in the lattice constant of Al-Ge mixtures was sufficient to explain the corresponding increase in T_c , without invoking any other enhancement mechanism.

C. Transition temperature versus grain size

In this section, the dependence of the transition temperature on the average grain size is presented and compared with the theoretical predictions of Parmenter,¹⁶ Hurault,¹⁷ and Garland *et al.*,²⁰ and compared with previous experimental studies.

Presented in Fig. 2 is a plot of $\ln \ln \alpha$ as a

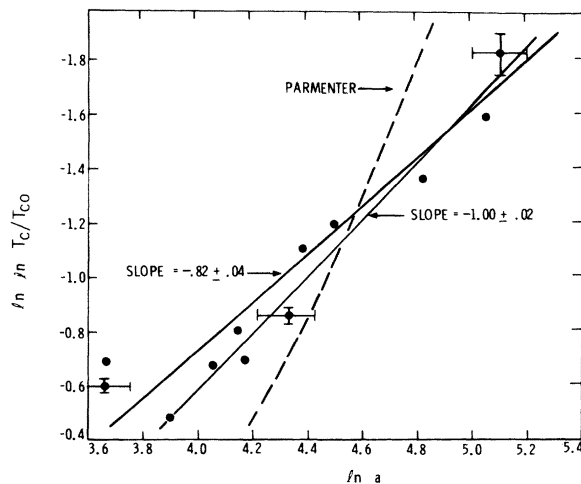


FIG. 2. Log-log plot of the enhanced transition temperature ratio T_c/T_{c0} as a function of the grain size. The dashed curve represents the theory of Parmenter discussed in the text.

function of $\ln a$. A least-squares straight-line curve fit to the data has a slope of -0.82 ± 0.04 . This indicates an approximate $1/a$ dependence for the increase in the transition temperature, in support of the picture of a soft phonon spectrum at the grain surface, which is producing the enhancement.^{17,18,20} It should be noted that the data for the three evaporation conditions all overlap.

The two experimental points for films Al 130 and Al 143 indicate a decrease in the transition temperature at very small grains ($\sim 40 \text{ \AA}$). Because of limited data at these small grain sizes, we cannot tell if this represents a true change in behavior. Only the theory of Garland *et al.* predicts an eventual decrease in the transition temperature at very small grains. Therefore, one should possibly compare other theories with our data both with and without these two data points. Neglecting the two films at $a = 40 \text{ \AA}$ gives a straight line slope of -1.00 ± 0.02 , exactly a $1/a$ dependence.

1. Comparison with the theory of Parmenter

As discussed in a previous section, by considering the quantization of electron levels in small grains, Parmenter¹⁶ calculated an enhanced critical temperature given by Eq. (1). Even though this equation predicts an initial dependence of $\ln \alpha$ on $1/a^3$, the dependence changes for large a . The slope of a $\ln \ln \alpha$ vs $\ln a$ curve, as predicted by Eq. (1), is given by

$$\frac{d \ln \ln \alpha}{d \ln a} = \frac{-3}{1 + \ln \alpha} \quad (6)$$

For the range of critical temperatures measured for our films, this slope varies from -1.9 at $T_c = 2.22 \text{ K}$ to -2.6 at $T_c = 1.41 \text{ K}$, with the average being ≈ -2.2 . Therefore, in the range of critical temperatures covered here, a plot of Eq. (1) will yield an approximate $1/a^2$ dependence (see Fig. 2).

The disagreement of Eq. (1) and our data as shown in Fig. 2 is quite evident. However, because of uncertainties in the absolute value of the measured grain sizes, our data can be shifted by a constant factor parallel to the $\ln a$ axis. In doing so, the slope remains unchanged and a better fit to the theoretical line is not achieved. Thus we conclude that the quantization of electron levels within a grain is not responsible for the enhancement in our films, which is consistent with the theoretical argument of Strongin *et al.*²⁴

2. Comparison with the theory of Hurault

Hurault¹⁷ considered two mechanisms for the enhancement of the critical temperature in small metallic particles: (i) A modified phonon spectrum at the surface of the crystal leads to an en-

hancement $\ln \alpha \propto 1/a$ while (ii) a polarizable coating surrounding each grain predicts an enhancement $\ln \alpha \propto 1/a^2$. Clearly, our data follow a $1/a$ dependence as previously described. In addition, no change in the behavior of $\ln \alpha$ to a $1/a^2$ dependence can be determined from the data. This rules out the second enhancement mechanism proposed above, even though the grains are coated with an oxide layer. This result is in accord with our earlier comments concerning the large band gap of the oxide. However, the oxide layer may further alter the phonon spectrum at the grain surface and thereby influence the magnitude of the enhancement.

The complete theoretical equation for the critical temperature as presented by Hurault for the first enhancement mechanism is

$$\ln \alpha = \left[\rho_0 \left(1 + \frac{\rho_0 a}{6(\rho_s - \rho_0) \delta a} \right) \right]^{-1} \quad (7)$$

where ρ_0 is the electron-phonon (el-ph) interaction parameter in bulk aluminum, and ρ_s is the el-ph interaction parameter in a thin surface layer of thickness δa surrounding a grain of diameter a . For bulk aluminum, $\rho_0 = 0.19$.² Fitting Eq. (7) to the data gives

$$(\rho_s - \rho_0) \delta a = 0.19 \text{ \AA} \quad (8)$$

Assuming that the surface layer thickness² $\delta a = 5 \text{ \AA}$ implies that ρ_s in the surface layer is increased to a value of 0.23.

3. Comparison with the theory of Garland *et al.* as modified by Watton

The theory of Garland *et al.*²⁰ explains the dependence of the critical temperature in thin films by considering the effect of lattice disorder. Starting with the equation

$$\ln \left(\frac{\langle \omega_{ph} \rangle}{T_c} \right) = \frac{1 + \lambda}{A(1 - \frac{1}{2} \mu^*) \lambda - \mu^*} \quad (9)$$

where $\langle \omega_{ph} \rangle$ is an average phonon frequency, λ is the electron-phonon coupling constant, A is a constant of the order unity and is crystal-structure dependent, and μ^* is the coulomb pseudopotential, they consider the effect of changes in $\langle \omega_{ph} \rangle$, λ , and A , represented by $\delta \langle \omega \rangle$, $\delta \lambda$, and δA , respectively, on the transition temperature. This leads to the equation

$$\ln \alpha = -\frac{1}{2} \frac{\delta \lambda}{\lambda} + \frac{1 + \lambda}{A(1 - \frac{1}{2} \mu^*) - \mu^*} - \frac{1 + \lambda(1 + \delta \lambda / \lambda)}{A(1 - \frac{1}{2} \mu^*) \lambda(1 + \delta \lambda / \lambda) [1 - \frac{1}{2} \beta(\delta \lambda / \lambda)] - \mu^*} \quad (10)$$

where

$$\delta \ln \lambda = -2\delta \ln \langle \omega_{ph} \rangle,$$

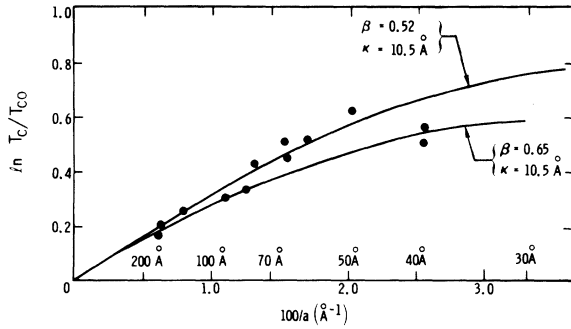


FIG. 3. Comparison of our data with the theory of Garland *et al.* for two values of β .

and

$$\delta \ln A = \beta \delta \ln \langle \omega_{ph} \rangle. \quad (11)$$

By fitting this expression to the experimental values for the enhanced transition temperatures of quenched films of Al and Pb, Garland *et al.* obtained a value for β of 0.52. This value depends upon the amount of lattice disorder, which may not be constant for our films. However, we have considered only the case where β is constant.

Watton⁵ has extended the above equation by applying a shell model to changes in λ at the grain surface. He assumed that

$$\lambda = \lambda_0 + (\lambda_s - \lambda_0) (6\delta a/a), \quad (12)$$

where as before λ_0 is the el-ph coupling constant in bulk aluminum, λ_s is the el-ph coupling constant in a thin shell of thickness δa surrounding a grain of diameter a . Thus

$$\frac{\delta \lambda}{\lambda} = \left(\frac{\lambda_s - \lambda_0}{\lambda_0} \right) \frac{6\delta a}{a} = \frac{\kappa}{a}, \quad (13)$$

where

$$\kappa = \left(\frac{\lambda_s - \lambda_0}{\lambda_0} \right) 6\delta a. \quad (14)$$

Substituting into Eq. (10) we have

$$\ln \alpha = -\frac{1}{2} \frac{\kappa}{a} + \frac{1 + \lambda}{A(1 - \frac{1}{2}\mu^*)\lambda - \mu^*} - \frac{1 + \lambda(1 + \kappa/a)}{A(1 - \frac{1}{2}\mu^*)\lambda(1 + \kappa/a)[1 - \frac{1}{2}\beta(\kappa/a)] - \mu^*}. \quad (15)$$

This equation is plotted in Fig. 3 for two values of β , with the value of κ chosen to give a best fit to the data. The agreement with the curve for $\beta = 0.52$ is quite good. Note that for a larger value of β , the maximum value of $\ln \alpha$ decreases and shifts to a smaller value of the grain size. For $\beta = 0.65$, the maximum agrees roughly with the maximum value obtained in our experiments, but is located at a grain size $a \approx 28 \text{ \AA}$, while our data

have a maximum at $a \approx 45 \text{ \AA}$. If β increases as the grain size decreases, one could possibly fit all of our data, including the two points at $a \approx 40 \text{ \AA}$. At present, it is unclear what the fundamental form for β should be, or what is its significance. However, the agreement with the theory of Garland *et al.*, as modified by Watton, also provides evidence that a change in the electron-phonon coupling at the surface of the grains is responsible for the observed enhancement in the critical temperature in our films.

4. Comparison with previous experiments

Several experiments by Watton⁵ have also found agreement with the theory of Garland *et al.*²⁰ In the case of aluminum, he found that

$$\ln \alpha \propto a^{-0.86}, \quad (16)$$

which agrees with our value of -0.82 . Because of this correspondence between our exponents, Watton's data can be made to fit our data by choosing the same value for a/κ at the same enhancement. However, since Watton was unable to measure the grain size directly, this correspondence does not imply the same value of κ for our experiments. A comparison would be most interesting, since in Watton's case there is probably very little oxygen in his films (the evaporation pressure was 10^{-9} Torr). A different value for κ could be directly attributed to the presence of the oxide layer in our films. A value for κ could have been obtained by Watton if at the last annealing temperature (room temperature) the grain size was measured with a technique such as the one we have used. In any case, assuming that we have the same value for κ implies that the grain size in Watton's films varied from 40 to 90 \AA .

The same enhancement mechanism found here was also found by Strongin *et al.*,¹¹ Deutscher *et al.*,⁶ and Naugle *et al.*¹³ This mechanism will also explain the results of Abeles *et al.*,¹² and Buckel and Hilsch,¹ since grain size variations for these films have already been established. However, this does not rule out another enhancement mechanism for films prepared in a different way. For example, the work of Hauser¹⁵ on Al-Ge sputtered films indicated that the enhancement was a result of changes in the bulk lattice constant. Under other evaporation conditions, a combination of several enhancement mechanisms may be important.

Our results indicate that $\ln \alpha$ is proportional to $a^{-0.82}$, in agreement with the work of Watton.⁵ This dependence of $\ln \alpha$ agrees with the theories of Garland *et al.*²⁰ and of Hurault.¹⁷ Both theories indicate that a change in the phonon spectrum of small crystallites is responsible for the increased transition temperatures in evaporated aluminum

films. Even though there is an oxide layer around each grain, the electron-exciton-electron enhancement mechanism proposed by Hurault¹⁷ is

not observed. The presence or absence of an oxide layer may only change the magnitude of the enhancement.

*Work performed at Cornell University under the support of the U. S. Energy Research and Development Administration. Use of the central facilities of the Materials Science Center at Cornell supported by the Advanced Research Projects Agency is also acknowledged.

- ¹W. Buckel and R. Hilsch, *Z. Phys.* **138**, 109 (1954).
²B. Abeles, R. W. Cohen, and G. W. Cullen, *Phys. Rev. Lett.* **17**, 632 (1966).
³M. Strongin and O. F. Kammerer, *J. Appl. Phys.* **39**, 2509 (1968).
⁴H. Bülow and W. Buckel, *Z. Phys.* **145**, 141 (1956).
⁵R. Watton, *J. Phys. C* **2**, 1697 (1969); *Solid State Commun.* **8**, 105 (1970).
⁶G. Deutscher, M. Gershenson, E. Grünbaum, and Y. Imry, *J. Vac. Sci. Tech.* **10**, 697 (1973).
⁷W. Ruhl, *Z. Phys.* **186**, 190 (1965).
⁸M. Strongin, O. F. Kammerer, D. H. Douglass, and M. H. Cohen, *Phys. Rev. Lett.* **19**, 121 (1967).
⁹F. R. Gamble and H. M. McConnel, *Phys. Lett. A* **26**, 162 (1968).
¹⁰F. Meunier, J. J. Hauser, J. P. Burger, E. Guyon, and M. Hesse, *Phys. Lett. B* **28**, 37 (1968).
¹¹M. Strongin, O. F. Kammerer, J. E. Crow, R. D. Parks, D. H. Douglass, and M. A. Jensen, *Phys. Rev. Lett.* **21**, 1320 (1968).
¹²P. N. Chubov, V. V. Eremenko, and Yu. A. Pilipenko, *Zh. Eksp. Teor. Fiz.* **55**, 752 (1968) [*Sov. Phys. - JETP* **28**, 389 (1969)].
¹³D. G. Naugle, J. W. Baker, and R. E. Allen, *Phys. Rev. B* **7**, 3028 (1973).
¹⁴A. Fontaine and F. Meunier, *Phys. Kondens. Mater.* **14**, 119 (1972).
¹⁵J. J. Hauser, *Phys. Rev. B* **3**, 1611 (1971).
¹⁶R. H. Parmenter, *Phys. Rev.* **154**, 353 (1967); **166**, 392 (1968).
¹⁷J. P. Hurault, *J. Phys. Chem. Solids* **29**, 1765 (1968).
¹⁸P. G. deGennes, *Rev. Mod. Phys.* **36**, 225 (1964).
¹⁹M. H. Cohen and D. H. Douglass, *Phys. Rev. Lett.* **19**, 118 (1967).
²⁰J. W. Garland, K. H. Bennemann, and F. M. Mueller, *Phys. Rev. Lett.* **21**, 1315 (1968).
²¹J. M. Dickey and A. Paskin, *Phys. Rev. Lett.* **21**, 1441 (1968).
²²M. Strongin, O. F. Kammerer, H. H. Farrell, and D. L. Miller, *Phys. Rev. Lett.* **30**, 129 (1973).
²³R. B. Pettit and J. Silcox, *J. Appl. Phys.* **45**, 2858 (1974).
²⁴M. Strongin, R. S. Thompson, O. F. Kammerer, and J. E. Crow, *Phys. Rev. B* **1**, 1078 (1970).
²⁵D. Allender, J. Bray, and J. Bardeen, *Phys. Rev. B* **7**, 1020 (1973).
²⁶J. J. Cowan and E. T. Arakawa, *Phys. Status Solidi* **1**, 695 (1970).
²⁷F. G. Brickweede, H. Van Dijk, M. Durieux, J. R. Clement, and J. K. Logan, *J. Res. Nat. Bur. Stand. A* **64**, 1 (1960).
²⁸L. G. Aslamazov and A. I. Larkin, *Fiz. Tverd. Tela* **10**, 1104 (1968) [*Sov. Phys. - Solid State* **10**, 875 (1968)].
²⁹W. E. Makser and R. D. Parks, *Phys. Rev. B* **1**, 2164 (1970).
³⁰A. K. Bhatnagar, P. Kahn, and T. J. Zammit, *Solid State Commun.* **8**, 79 (1970).
³¹B. Abeles, R. W. Cohen, and W. R. Stowell, *Phys. Rev. Lett.* **18**, 902 (1967); R. W. Cohen and B. Abeles, *Phys. Rev.* **168**, 444 (1968).
³²J. J. Hauser, *J. Low Temp. Phys.* **7**, 335 (1972).
³³M. Levy and J. L. Olsen, in *Physics of High Pressures and Condensed Phase*, edited by A. Van Itterbeek (North-Holland, Amsterdam, 1965), Chap. 13.